The Uncertainty of Rock Mass Shear Strength Estimates: How to Incorporate the Reduction in Variance Due to Spatial Averaging for Use in Probabilistic Analysis

S.D. Cylwik Call & Nicholas, Inc., U.S.A.
J.A. Beck Call & Nicholas, Inc., U.S.A.
T.M. Ryan Call & Nicholas, Inc., U.S.A.

ABSTRACT

Rock mass strength is typically estimated from three fundamental components: intact rock strength, fracture strength, and intensity of fracturing. The uncertainties regarding the estimation of rock mass shear strength can also be separated into three distinct components: natural variability, statistical uncertainty, and transformation uncertainty. The natural spatial variability of geologic materials typically has the greatest impact on the uncertainty of rock mass design parameters. If the spatial continuity (autocorrelation) of input variables is not considered, a probabilistic slope analysis can result in either over- or under-estimation of the probability of failure. It is well established that the stability of a slope is controlled by the total shear resistance along the failure surface, rather than the shear resistance at any one individual location. For probabilistic slope analysis, it is therefore appropriate to determine the variance of the rock mass strength over the entire potential zone of failure. The variance of the shear strength across the failure surface will always be less than the variance of individual small-scale measurements of shear strength at any one location on that surface. The scale of fluctuation of each of the three components of rock mass strength (intact strength, fracture strength, intensity of fracturing) must be considered in order to estimate the variance of rock mass strength over the failure surface area. Intact rock strength and fracture strength typically exhibit a small spatial correlation distance relative to typical open pit slope analysis. Therefore, it is proposed that the natural variability for these parameters can be disregarded and in most cases only the statistical uncertainty of intact and fracture shear strength derived from the total population of representative laboratory tests need to be considered. Conversely, intensity of fracturing, as measured by either RQD or the GSI structure rating, tends to exhibit large spatial correlation distances relative to typical sampling intervals. A variogram model can be used in conjunction with the variance reduction function to characterize the spatial variability of the fracture intensity and to quickly estimate the reduced variance due to spatial averaging for use in probabilistic analysis. Examples are provided to demonstrate the value of these concepts.

1. INTRODUCTION

Accurate evaluation of risk is a fundamental challenge that all geotechnical engineers encounter. The high levels of uncertainty associated with in situ geological materials are what differentiate geotechnical engineering from other disciplines. Unstable geotechnical structures may cause injury to persons, operational delays, and/or expenses for repair. Traditional geotechnical analyses utilize deterministic methods to estimate a factor of safety (FOS), which is defined as the ratio of resisting forces to applied loads. However, the factor of safety is not a consistent measure of risk (Li and Lumb, 1987); a large range of risk levels may exist for the same factor of safety value. An alternative to deterministic analysis is to model important parameters as random variables and estimate a probability of failure. The probability of failure (P_f) is defined as the probability that the factor of safety is less than unity. Probabilistic methods are becoming more commonplace in geotechnical practice as they permit financial and safety evaluations to be addressed quantitatively.

1.1 THE EFFECT OF SPATIAL AVERAGES IN PROBABILISTIC ANALYSIS

Virtually all geotechnical properties are of some type of local spatial average (Fenton and Griffiths, 2008). Even a laboratory compression test measures the average bond strength of the sample throughout the failure region, not the strength at any one single point. Similarly, the stability of a slope is controlled by the total shear resistance along the failure surface, rather than the shear resistance at any individual location. The 'point-to-point' variability of shear strength that is estimated directly from geotechnical tests is typically of very little use to geotechnical engineers (Li and Lumb, 1987; Vanmarcke, 2010).

To demonstrate the effect spatial averaging has on a parameter, let us assume that a random variable u varies with distance x, as presented in Figure 1. The spatial average of the property $u(x)$ over the interval T may be written as:

$$u_T(x) = \frac{1}{T}\int_T u(x)\,dx \approx \frac{1}{T}\sum_{x-T/2}^{x+T/2} u(x) \tag{1}$$

Where:

u(x)	=	random variable *u* as a function of *x*
$u_T(x)$	=	moving spatial average of function *u(x)* over interval size *T*
T	=	size of spatial average

The integrand is used for continuous fields of data, whereas the summation must be applied to discontinuous data fields as are typically encountered in geotechnical engineering. Note that spatial averaging has no effect on the mean value of parameter *u* (Vanmarcke, 2010); however, the variance of the parameter is significantly reduced. The process of spatial averaging reduces the variance because fluctuations cancel out during the averaging process and deviations from the mean become less extreme.

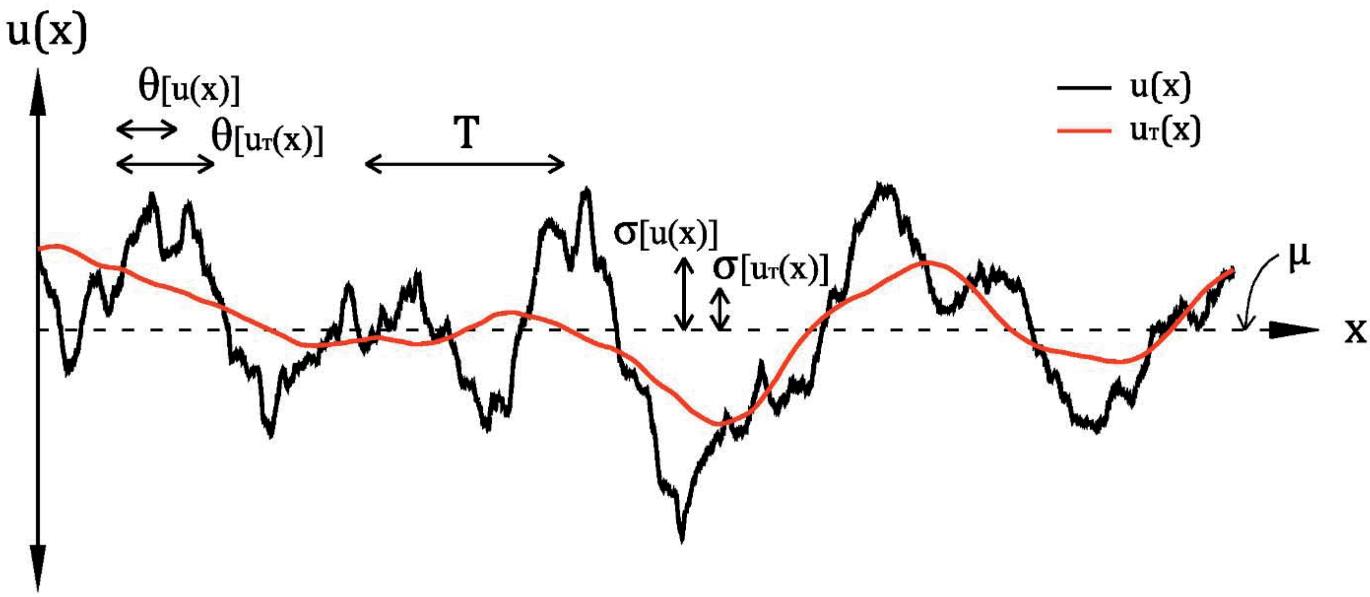

Figure 1 Graph of function u(x) and its spatial average over T, $u_T(x)$

Unintended effects occur when the variance of shear strength is not adjusted for model zone size in a slope analysis. Consider a 500-meter high rock slope cut at 45 degrees analyzed by two-dimensional probabilistic limit-equilibrium methods with Monte Carlo sampling, as shown in Figure 2. Three cases are considered, each with identical rock-mass properties (same μ and σ of unit weight, cohesion, and friction angle with a normal distribution). The only variation between the analyses is the number of geotechnical domains modeled (and therefore, the number of independent distributions sampled). All three cases result in the same FOS value as expected, however the estimated P_f varies by a factor of eight. Following this logic, if a practitioner wishes to significantly lower the estimated P_f he or she must only create a geotechnical model with more material subdivisions. As the number of independent distributions sampled increases, the probability of the average strength along the critical slip surface deviating significantly from the mean decreases; the spatial averaging of the additional distributions will tend to cancel out fluctuations. To properly estimate P_f, the variance of the parameters must be adjusted based on the spatial extent of the zone being analyzed. The appropriate standard deviation for a geotechnical parameter is directly related to the size of the model zone (i.e., the size of the spatial average).

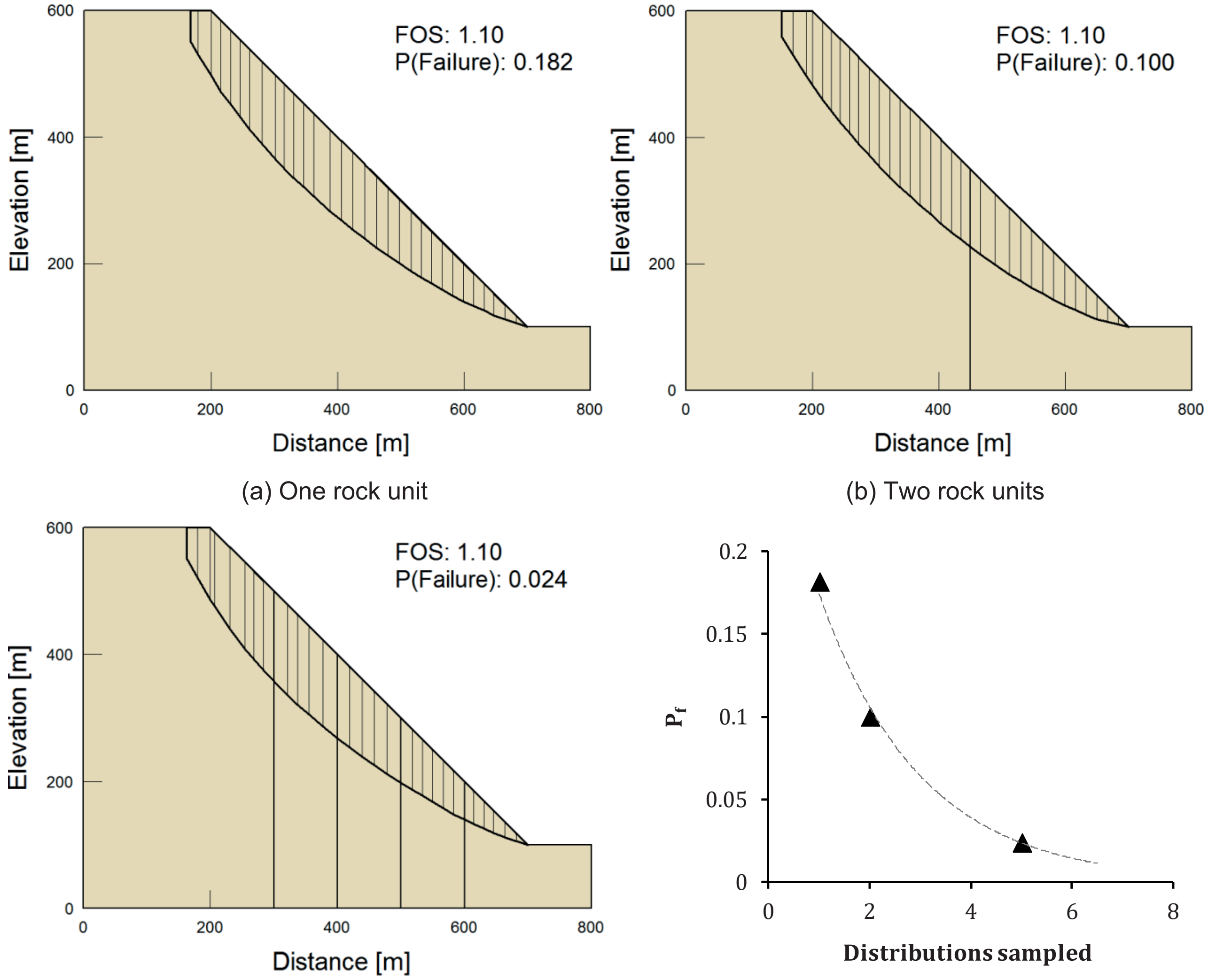

(a) One rock unit

(b) Two rock units

(c) Five rock units

(d)

Figure 2. Limit equilibrium analysis of a 500-meter high 45-degree slope with properties unit weight μ=26.5 kN/m3 σ=0, cohesion μ=360 kPa σ=40 kPa, and friction angle μ=33 degrees σ=2 degrees, sampling a) One rock unit, b) Two rock units, c) Five rock units, and d) Plot of probability of failure versus number of distributions sampled

In order to quantify and predict the reduction in variance due to spatial averaging, an additional parameter is required beyond the mean and variance. The parameter is called the *scale of fluctuation* (θ) (or correlation distance), and defines the distance of spatial correlation, or the distance within which the parameter shows relatively strong correlation and beyond which shows no correlation (Vanmarcke, 2010). It characterizes how rapidly the property varies in space. Two points that lie within a distance of θ are likely either to be both above, or both below the mean value. The θ value is synonymous with the 'range' parameter familiar to geostatisticians.

The scale of fluctuation can be roughly estimated from a one-dimensional line plot as the average distance between intersections of the fluctuating property and its mean multiplied by 1.25 (Vanmarcke, 2010). For example, in Figure 1 there are twelve total mean crossings of the function u(x) (black line). This method of estimating θ becomes more challenging in three dimensions when discontinuous and randomly spaced data fields are encountered as is typical in geotechnical data; more robust estimation methods are described in the following sections.

The θ value can be used in conjunction with the variance reduction function to quickly estimate the reduced variance due to spatial averaging for use in probabilistic analysis. Combined with the two other sources of uncertainty (statistical and transformation), the variability of rock mass strength can be estimated for use in geotechnical analysis.

2. SOURCES OF UNCERTAINTY

In a probabilistic analysis, rock mass parameters are modeled as random variables so that the full range of possible outcomes may be investigated. Three distinct components contribute to the total uncertainty of a rock mass parameter estimate: natural variability, statistical uncertainty, and transformation model uncertainty, as summarized in Figure 3.

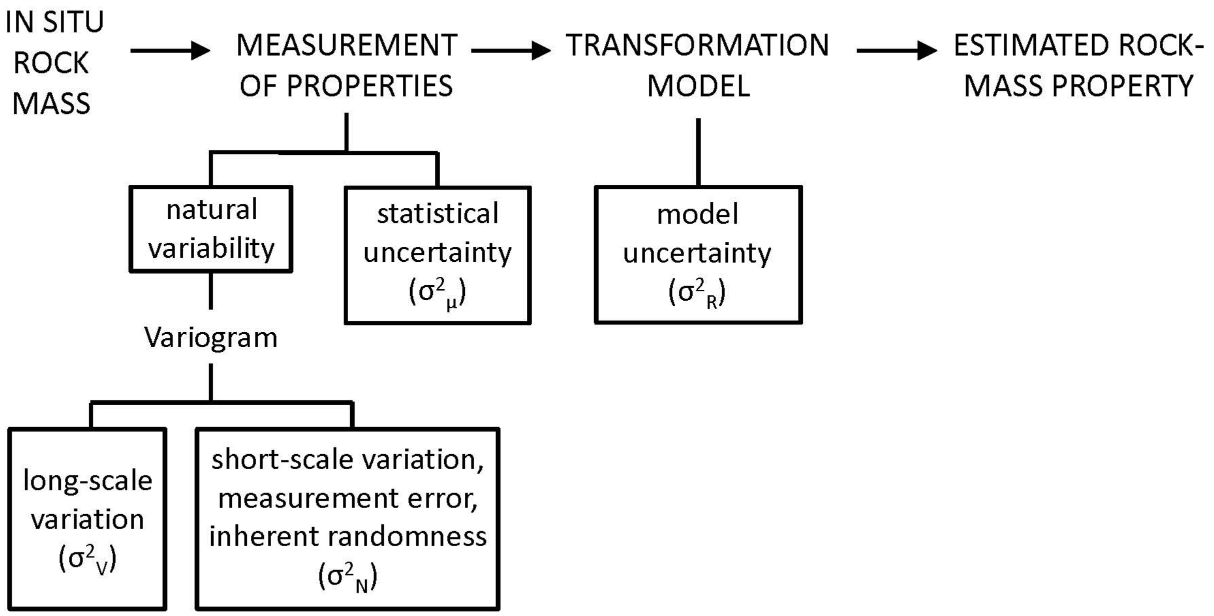

Figure 3 Sources of uncertainty in rock-mass property estimates (after Phoon and Kulhawy, 1999)

The uncertainty of each rock-mass input parameter must be quantified independently before a transformation model is applied to estimate the desired rock mass property. The total variance of an input parameter (σ^2_{input}) is estimated using equation 2, where $\Gamma^2(A)$ is the variance reduction function evaluated over area *A* (or if applicable, over a length or volume), σ^2_V is the long-scale variance, and σ^2_μ is the variance of the mean. The variance reduction function ranges from 0 to 1, and converts the 'point-to-point' variance to the variance of a spatial average over area *A*.

$$\sigma^2_{input} = \Gamma^2(A) \cdot \sigma^2_V + \sigma^2_\mu \qquad (2)$$

The total variance of a rock mass parameter is dependent upon the variance of each input parameter (estimated with equation 2) and of the uncertainty of the transformation model itself (σ^2_R), as summarized in Figure 4.

The three different sources of uncertainty are defined and discussed in the following sections.

$$\begin{matrix} \sigma^2_{input\ 1} \\ \sigma^2_{input\ 2} \\ \ldots \end{matrix} \rightarrow \begin{matrix} \textit{Randomly sample input} \\ \textit{parameters to estimate } \sigma^2 \\ \textit{of rock mass parameter} \end{matrix} \rightarrow \begin{matrix} \textit{Apply transformation} \\ \textit{model variance of } \sigma^2_R \end{matrix} \rightarrow \begin{matrix} \sigma^2 \textit{ of rock mass} \\ \textit{parameter} \end{matrix}$$

Figure 4. Workflow to determine variance of a rock mass parameter

2.1. NATURAL VARIABILITY

Natural variability is the in situ variation of geological properties from one point to another, and is also referred to as spatial variability, inherent variability, or simply 'data scatter.' Univariate statistics are the primary method to evaluate and describe the natural variability of a dataset; examples of univariate statistical analysis include the mean, median, standard deviation, and frequency histogram.

Univariate statistics reveal the measured distribution of values, but tell us nothing of how the measured property varies through space. Figure 5 presents two different two-dimensional data fields (modeled after El-Ramly et al., 2002) of the rock-mass index parameter GSI (geological strength index) (Hoek et al., 2002). The data sets have nearly identical univariate statistics of μ, σ, and frequency distribution (shown on left), however, their spatial distribution of values is drastically different. The θ distance is significantly larger for case B (the zones of high and low values are much larger in case B). If an analysis for a tunnel excavation was conducted for each case, the P_f would be higher for a tunnel excavated in case B than case A since the probability of encountering a large zone in which the majority of GSI values are below the mean is significantly greater for case B.

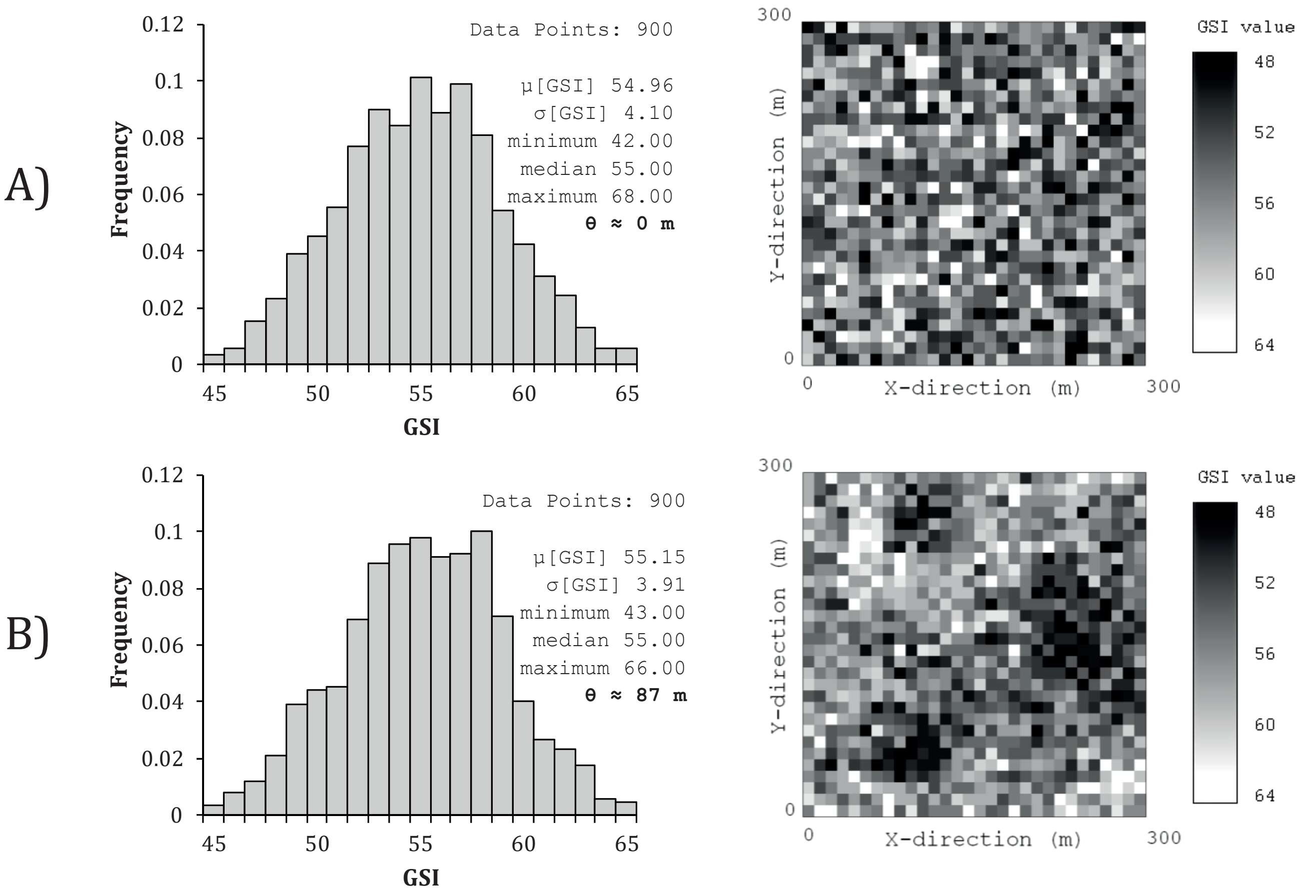

Figure 5. Two random fields of GSI with different spatial distribution properties but similar mean, point standard deviation, and probability density function

2.1.1 Spatial Characterization of Natural Variability Using the Variogram

The variogram (also referred to as the semi-variogram) allows us to evaluate not just the value of a measurement, but also the location of that measurement. The variogram describes how related (correlated) data points are to each other at different separation distances, referred to as 'lag' distances. It is a measure of dissimilarity, where a result of zero implies perfect correlation and increasing variance values indicate less correlation. The variogram is the preferred simple estimator of spatial continuity because it is unbiased and does not require any assumptions about the dataset – unlike the autocorrelation function, which requires an estimate of the mean in order to calculate (Fenton and Griffiths, 2008).

Geotechnical data is usually first grouped into lag 'bins' of similar separation distance; this is required because geotechnical data is often spaced at irregular intervals. The tolerance limits on the bins should be small enough to maintain resolution of the variogram, yet large enough so that the variogram shape is stable (Cressie, 1991). The experimental variogram of the random variable *u* at lag bin distance τ is defined as:

$$\gamma(\tau) = \frac{1}{2N}\sum_{i=1}^{N}[u(x) - u(x+\tau)]^2 \quad (3)$$

where N represents the total number of data pairs within the specified lag distance tolerance.

Once the experimental variogram is calculated, a model variogram is fit to the experimental data. A continuous variogram model is required for variance reduction calculations and also for spatial interpolation (kriging). In the author's experience, most geotechnical data fits very well to the exponential variogram model, which is defined as:

$$\gamma(\tau) = \sigma_N^2 + \sigma_V^2\left(1 - e^{-\frac{2|\tau|}{\theta}}\right) \quad (4)$$

An example experimental data set and exponential variogram model are shown in Figure 6. The lag distance and semi-variance has been normalized to make the plot universal.

A typical variogram may be described by the following components:

- The Scale of Fluctuation (θ). The lag distance within which the parameter shows relatively strong correlation and beyond which shows very low correlation. It is approximately the lag distance at which the variance no longer increases, or, 'levels off.' The θ distance is synonymous with the 'range' parameter familiar to geostatisticians. A flat variogram implies that either the data is not spatially correlated, or it is correlated only at distances smaller than the closest sample spacing.
- The Sill ($\sigma^2_N + \sigma^2_V$) is the semi-variance that is measured when only data pairs separated by large enough lag distances to be considered independent are compared. Data pairs separated by this distance or greater are no longer correlated. Once the sill is reached, data points separated by this distance are effectively 'independent' from each other.
- The Nugget (σ^2_N) is the vertical axis intercept of the variogram at a lag distance of zero. The 'nugget effect' can be induced by many different sources: correlation at distances smaller than the closest sample spacing (short-scale variation), measurement error, positional error, or inherent randomness. Under normal circumstances, it is not possible to determine which source or combination of sources causes the nugget effect. Very smooth data fields tend to have a small nugget value, and erratic data fields a large nugget value. The term nugget effect is said to originate from the micro-variability caused by one grade sample that could contain a gold nugget, while the sample directly adjacent to it could be barren and therefore cause high semi-variance at small lags.

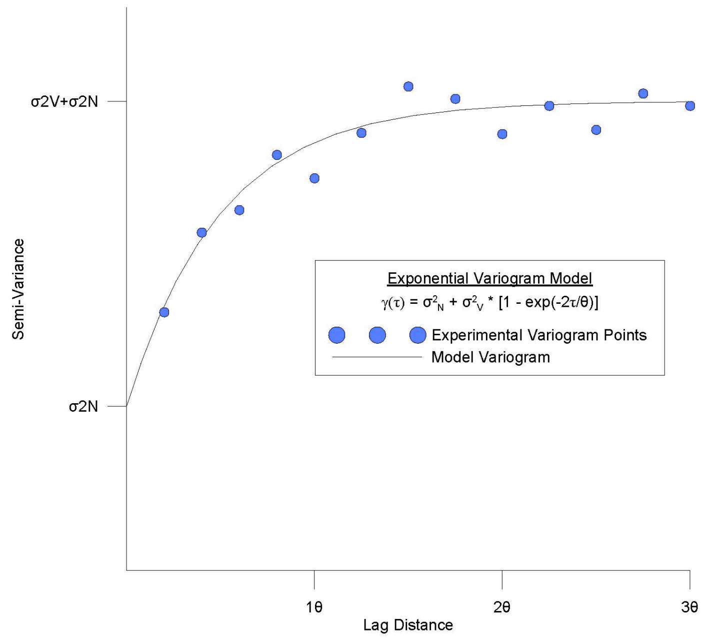

Figure 6. Example of the exponential variogram model with nugget effect

2.1.2. The Variance Reduction Function

As discussed in Section 1.0, the variance of a parameter is reduced as the size of the spatial average of that parameter increases. The maximum variance is obtained with the 'point-to-point' estimate, and the variance approaches zero as the spatial average size grows to infinity; however, we are typically interested in the value of the variance in between these two cases. The dimensionless function $\Gamma^2(T)$ defines the reduction of the point variance (σ^2) due to a spatial average of length *T*. The variance reduction function lies between 0 and 1, has a value of 1.0 when *T* = 0, and approaches zero as *T* increases (Vanmarcke, 2010; Fenton and Griffiths, 2008). The concept of variance reduction due to spatial averaging is synonymous with the 'change of support' concept familiar to resource geologists.

The variance function for a one-dimensional process can be calculated as follows (Vanmarcke, 2010):

$$\Gamma^2(T) = \frac{1}{T^2}\int_0^T\int_0^T \rho(\tau_1 - \tau_2)d\tau_1 d\tau_2$$

(5)

Where ρ(τ) is the correlation function, which for a 'spatially homogeneous' and stationary random field is related to the variogram by the following:

$$\rho(\tau) = 1 - \frac{\gamma(\tau)}{\sigma^2}$$

(6)

Conversely, the correlation function may be derived from the variance function with the derivative:

$$\rho(\tau) = \frac{1}{2}\frac{d^2}{d\tau^2}[\tau^2\Gamma^2(\tau)] \qquad (7)$$

The variance reduction function for the exponential variogram model (equation 4) can be written:

$$\Gamma^2(T) = 2\left(\frac{\theta}{2T}\right)^2\left(\frac{2T}{\theta} - 1 + e^{-2T/\theta}\right) \quad T > 0$$

(8)

For the exponential model, the only inputs to the variance function are θ and *T*. If we have a variogram model, we can now calculate the reduced variance, σ^2_T, for any size one-dimensional spatial average, *T*:

$$\sigma_T^2 = \Gamma^2(T)\cdot\sigma_V^2 \quad T > Sampling\ Interval \qquad (9)$$

Note that the full measured variance of a parameter (σ^2, equal to $\sigma^2_V + \sigma^2_N$) is not present in equation 9. A notable finding of the variance function is that a spatial average of any size will theoretically reduce the nugget variance (σ^2_N) to zero; this implies that the components of the variance that originate from high frequency fluctuations and inherent randomness will be 'averaged out' so long as the spatial average size is larger than the sampling interval of the data that was used to generate the variogram model. The other components that contribute to the nugget variance, measurement error and positional error, are *not* representative of actual in situ variation and therefore it is also not desirable to include them in estimates of variability for a probabilistic geotechnical model. For some projects, eliminating the nugget variance will significantly reduce the design variance used for analysis.

A multi-dimensional variance function can be expressed as the product of multiple one-dimensional variance functions as follows (Vanmarcke, 1977):

$$\Gamma^2(x,y,z) = \Gamma^2(T_x)\,\Gamma^2(T_y)\Gamma^2(T_z) \qquad (10)$$

Each factor in equation 10 is the one-dimensional form of the variance function shown in equation 8, where x, y, and z represent the side lengths of a rectangular box. The exponential variance functions for one, two and three dimensions are plotted in Figure 7. The spatial average size and variance has been normalized to make the plot universal. Note that the variance is reduced more quickly as the number of dimensions of the spatial average increases.

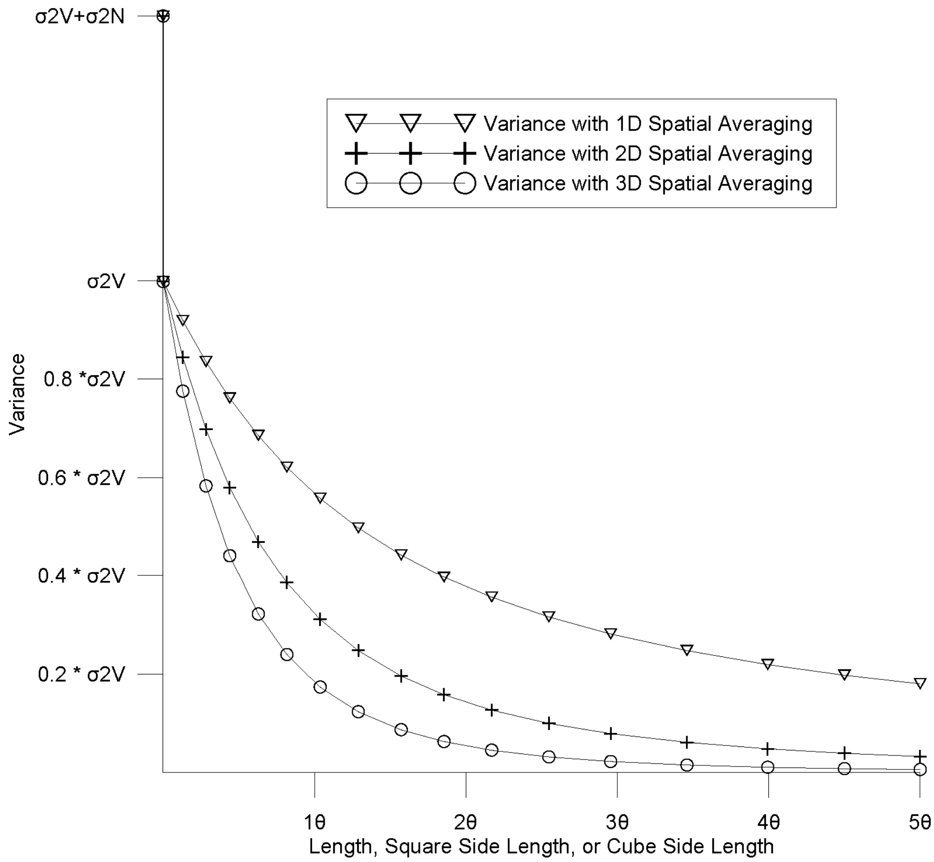

Figure 7. One-, two-, and three-dimensional variance functions for the exponential model

2.2. STATISTICAL UNCERTAINTY

When data is limited, it is important to recognize that our estimation of the mean is itself a random variable. It is quite common in geotechnical engineering to only sample a very small portion of the population. Therefore, it is necessary to assess how accurate our estimation of the mean actually is relative to the true population mean. The variance and standard deviation of the sample mean estimate are defined as follows (Ang and Tang, 1975):

$$\sigma_\mu^2 = {\sigma^2}/{n} \qquad \sigma_\mu = {\sigma}/{\sqrt{n}} \tag{11}$$

As the total number of samples (n) is increased, eventually the mean of the samples will converge on the true mean of the population. The above equations assume that all samples are independent from each other; however, as demonstrated by the variogram, samples near each other might in fact be correlated. If the samples are correlated to one another, the uncertainty of the estimated mean will actually be significantly greater than equation 11 would indicate. Fortunately, so long as the sampling domain size is significantly larger than θ, the above equations remain valid estimators.

2.3. TRANSFORMATION UNCERTAINTY

It is difficult to directly measure rock mass strength (geotechnical tests are typically not representative of in-situ rock mass strengths), and most practitioners therefore employ a transformation model to estimate rock mass strength from parameters that are more easily measured. Transformation models select the most important/abundant parameters as inputs, and then apply an empirical transform to estimate rock mass strength. Examples of transformation models are the Hoek-Brown strength criterion (Hoek et al., 2002) and the CNI modulus reduction method (Call et al., 2001; Read and Stacey, 2009). Transformation models provide *approximations* of the true rock mass strength. Even with an unlimited geotechnical budget, the true rock mass strength could never be determined with absolute certainty because of the simplifications that are required to make a transformation model practical; a transformation model would not prove useful if every parameter that affected rock mass strength was required as an input. For example, two different rock masses could have the same GSI, uniaxial strength, and m_i value, and we would still expect that their true in situ shear strengths not be exactly the same because of transformation uncertainty.

Transformation uncertainty may be estimated with the coefficient of variation (COV), which scales the standard deviation by the mean:

$$\sigma_R = \mu \cdot COV_R \tag{12}$$

Researchers have estimated COV_R values between 10 and 35 percent for geotechnical transformation models (Wiles, 2006; Phoon and Kulhawy, 1999). Exact COV_R values are not known. It is advisable to select a higher COV_R value for greenfield sites where experience is limited. For well-developed projects with calibration of previous excavation performance, lower values of COV_R may be appropriate.

3. SPATIAL CORRELATION OF ROCK MASS PARAMETERS

The properties of each input parameter to the rock mass strength transformation model must be evaluated separately. The input parameters are separated into two groups: intact and fracture strength, and intensity of rock-mass fracturing.

3.1. SPATIAL CORRELATION OF INTACT AND FRACTURE STRENGTH

The spatial variability of strength testing data from multiple projects were evaluated to determine typical θ values for intact and fracture shear strength. A summary of the datasets evaluated is shown in Table I and the variograms are plotted in Figure 8. Most of the variograms exhibit 'pure nugget effect' (a flat, horizontal variogram line), which implies that θ is smaller than the closest sampling distance. The only project with an interpretable variogram is the Yima North dataset (Wang et al., 2000) with a measured θ of 9 meters. Other studies have also found large nugget effects, but sometimes with large θ values (Mayer and Stead, 2017).

When the θ distance is significantly smaller than the slope being analyzed, a multitude independent samples will be averaged together over the failure zone, significantly reducing the natural variability variance (σ^2_V). For example, if we assume a θ of 9 meters and that the nugget variance is equal to 50 percent of the total variance (properties of the Yima North sandstone), only a 14-meter spatial average in two dimensions or an 8-meter spatial average in three dimensions is required to reduce the measured σ^2_V by 90 percent (using equations 8, 9, and 10). Recall that the nugget variance (σ^2_N) is reduced to zero for any nominal spatial average size larger than the sample spacing (section 2.1.2).

It is proposed that the natural variability of intact and fracture shear strength can be disregarded in most cases when the slope height under investigation is significantly greater than θ. The statistical uncertainty (variance of the mean) must still be considered even if natural variability is not. A limited budget is typically available for geotechnical testing, and therefore the variance of the mean is often of significance for intact and fracture shear strength uncertainty estimates. Notwithstanding, if sufficient data is present to plot the variogram for a specific project, it should be verified that θ is indeed very small relative to the slope analysis.

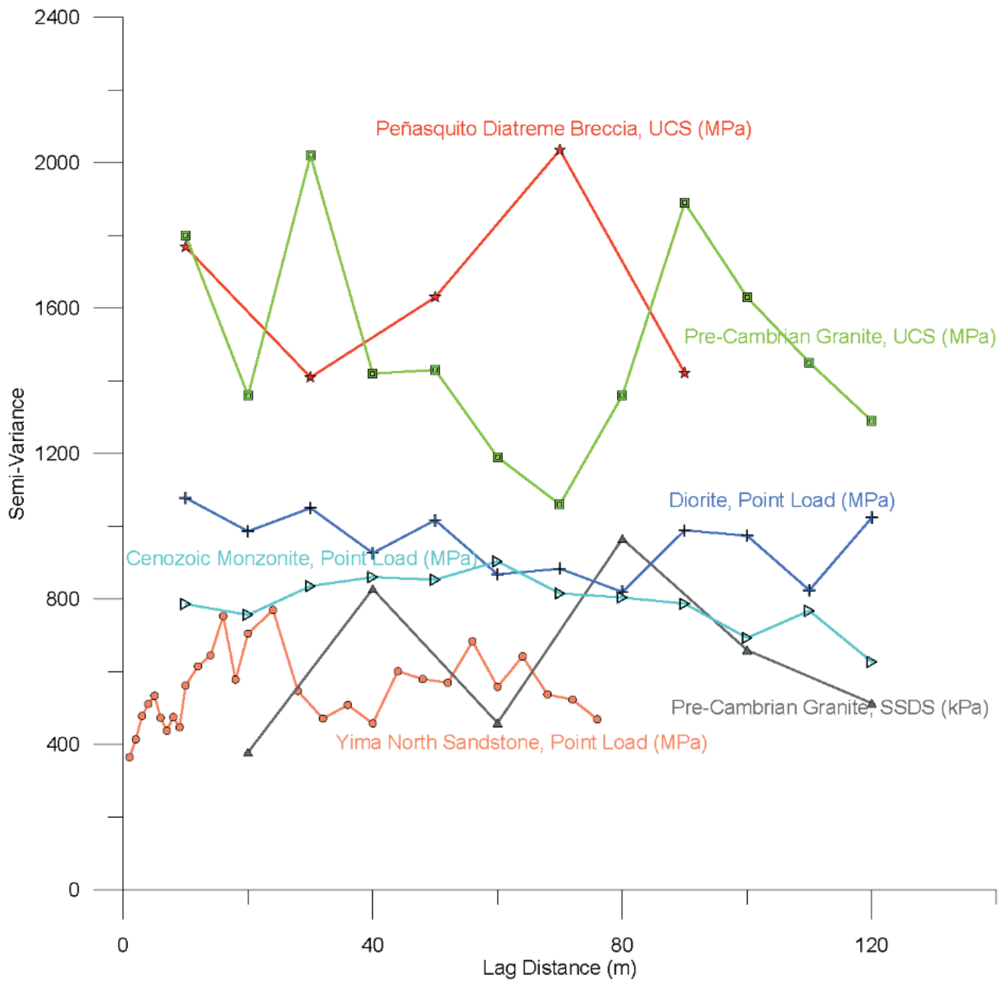

Figure 8. Variograms of intact and fracture shear strength testing data

Table I Summary of intact and fracture direct shear data

Project	Lithology	Test Type	Number of Tests	Mean	Variance	Unit of Variance	θ
Yima North	Sandstone	Point Load	100	32.5	570	MPa (Is50 * 24)	9 m
Chilean Mine	Diorite	Point Load	339	130.9	2 460	MPa (Is50 * 24)	< 10 m
Peñasquito	Diatreme Breccia	UCS	53	159.2	1 907	MPa	< 10 m
SW USA	Cenozoic Monzonite	Point Load	308	43.2	790.2	MPa (Is50 * 24)	< 10 m
Copper-	Pre-Cambrian Granite	UCS	396	92.5	2 055	MPa	< 10 m
Porphyrys	Pre-Cambrian Granite	SSDS	70	239.8	966	kPa (τ @ 300 kPa σ_n)	< 20 m

3.2. SPATIAL CORRELATION OF FRACTURE INTENSITY (RQD)

Parameters that quantify fracture intensity, such as RQD (rock quality designation) (Deere, 1968) or the GSI structure rating, often demonstrate sufficient spatial correlation to create interpretable and useful variogram models. RQD is most often utilized for variography since these data are recorded at most sites, and can also be used to estimate other rock-mass parameters such as fracture frequency or the GSI structure rating (Palmstrom, 2005; Hoek et al., 2013). So long as RQD values are either weighted by the drill interval length or composited into intervals of equal length, it is valid to arithmetically average RQD values.

3.2.1 Example Variograms – Granite Pluton

The RQD database from a Cretaceous age granite pluton located at a North American mine is used to demonstrate typical variograms of fracture intensity. The three-dimensional isotropic experimental variograms for the granite are presented in Figure 9. Three geotechnical domains have been identified in the granite and so the experimental variogram is calculated for each separately. An exponential variogram model is fit to domain #2 (argillic altered granite) for the purposes of this example, as shown in Figure 9. Note that the nugget variance accounts for about 35 percent of the total variance, and the modeled θ is 28 meters.

4. PRACTICAL APPLICATION FOR A LIMIT-EQUILIBRIUM ANALYSIS

The data from the granite domain #2 is used to demonstrate the workflow for a two-dimensional limit-equilibrium slope analysis with consideration of the effects of spatial averaging.

4.1. ESTIMATION OF MEAN ROCK-MASS STRENGTHS

The measured intact, fracture, and RQD properties of the argillic altered granite (domain #2) are shown in Table II. We will assume that the θ value of intact and fracture strength parameters is small relative to the size of the slope, and therefore only the standard deviation of the mean is required (Section 3.1). The mean RQD in domain #2 is 24.4 percent.

For this example, the rock mass strength is estimated using CNI modulus reduction method (Call et al., 2001; Read and Stacey, 2009). The Hoek-Brown method could also be used. The CNI method is defined by the following equations, with coh_{intact} and phi_{intact} estimated from uniaxial and triaxial tests and $coh_{fracture}$ and $phi_{fracture}$ estimated from small scale direct shear tests of natural fractures:

$$coh_{rock\ mass} = \gamma[r^2 coh_{intact} + (1 - r^2)coh_{fracture}] \quad (13)$$

$$phi_{rock\ mass} = \text{atan}[r^2 \tan(phi_{intat}) + (1 - r^2)\tan(phi_{fracture})] \quad (14)$$

$$r = \alpha e^{\beta \cdot RQD} \quad (15)$$

$$for\ cohesion, \qquad \alpha = 0.225\ \ and\ \beta = 0.013,\ \ \gamma = 0.5$$

$$for\ phi, \qquad \alpha = 0.3775\ \ and\ \beta = 0.0075$$

For the granite domain #2 properties the estimated mean rock mass strength is:

$$coh_{rock\ mass} = 197.2\ kPa$$

$$phi_{rock\ mass} = 23.5\ degrees$$

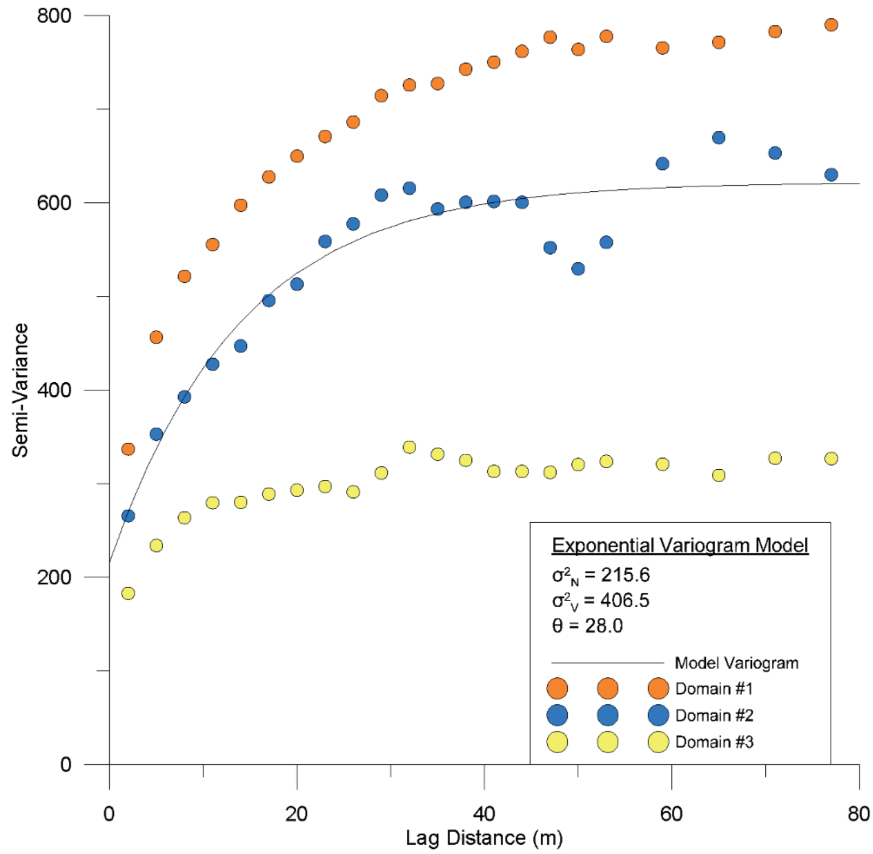

Figure **9. Variograms of RQD data for the granite pluton at a gold mine**

Table II. Summary of measured intact, fracture, and RQD properties

Rock Type	Intact rock strength				Fracture strength				RQD			
	coh [kPa]		phi [deg]		coh [kPa]		phi [deg]			Variogram Model		
	μ	σ_μ	μ	σ_μ	μ	σ_μ	μ	σ_μ	μ	θ [m]	σ^2_N (σ_N)	σ^2_V (σ_V)
Granite Domain #2	3740	1509	33.6	3.5	41.4	6.6	20.6	2.1	24.4	28.0	215.6 (14.68)	406.5 (20.16)

4.2. ESTIMATION OF VARIABILITY OF ROCK MASS STRENGTH

Since rock mass strength may not be measured directly, distributions of measurable rock properties must be randomly sampled to generate the expected distribution of rock mass strength. Considering that any spatial average will reduce the nugget variance to zero, only the variance of the mean is required to define the variability of intact and fracture strength. The RQD database for granite domain #2 contains thousands of drill intervals and therefore the variance of the mean is assumed to be zero. The variance reduction function (equations 8 and 10) is used to reduce the long-scale variation of the RQD based on the spatial average size; it is assumed that the spatial average length along the slip surface is equal to the height of the slope (h), and that the width of the slip surface (w) is equal to half of the slope height, or:

$$\sigma^2_{T-RQD} = \sigma^2_V \Gamma^2(h)\, \Gamma^2(w) \qquad (16)$$

The results of the variance reduction of RQD for various slope heights between 40 and 180 meters are presented in Table III. The estimated variance and standard deviation values for the rock-mass strength by slope height (considering the measured intact, fracture, and RQD properties of the granite presented in Table II) are also shown in Table III. All input parameters were assumed to follow the log-normal distribution, and the RQD values were limited to a maximum value of 100. The sampled rock mass strength friction angles were not permitted to go below the measured fracture shear strength (20.6 degrees) since this defines the potential lower limit of the rock-mass strength. A transformation model COV_R of 0.1 was assumed to arrive at the final estimated rock-mass strength variances shown on the far right in Table III. Note how the predicted variability of the rock-mass strength is reduced as the slope height grows larger.

Table III. Summary of estimated rock mass strength variability by slope height

Slope Height (m)	$\Gamma^2(h)$ (eq. 8)	$\Gamma^2(w)$ (eq. 8)	$\sigma^2_{T\text{-}RQD}$ ($\sigma_{T\text{-}RQD}$) (eq. 16)	Predicted variability of rock-mass strength: Before application of σ_R — σ^2 (σ) of coh (kPa)	σ^2 (σ) of phi (deg)	Corr. Coeff. (coh-phi)	After σ_R (eq. 12) — σ^2 (σ) of coh (kPa)	σ^2 (σ) of phi (deg)
40	0.469	0.655	125 (11.2)	11700 (108.2)	3.61 (1.90)	0.19	16360 (127.9)	18.1 (4.25)
60	0.359	0.549	80.2 (8.95)	8460 (91.98)	3.50 (1.87)	0.13	12480 (111.7)	17.8 (4.22)
90	0.263	0.436	46.6 (6.83)	6754 (82.19)	3.39 (1.84)	0.07	10390 (101.9)	17.6 (4.19)
120	0.206	0.359	30.1 (5.49)	6135 (78.32)	3.35 (1.83)	0.05	9613 (98.05)	17.5 (4.18)
180	0.143	0.263	15.3 (3.91)	5700 (75.50)	3.35 (1.83)	0.02	9067 (95.22)	17.5 (4.18)

4.3. LIMIT-EQUILIBRIUM ANALYSIS RESULTS

Two-dimensional limit-equilibrium analysis was performed for the slope heights listed in Table III with slope angles of 35, 45, and 55 degrees. The FOS and P_f values are plotted against the slope height in Figure 10. As expected, the FOS decreases with slope height and the P_f increases with slope height.

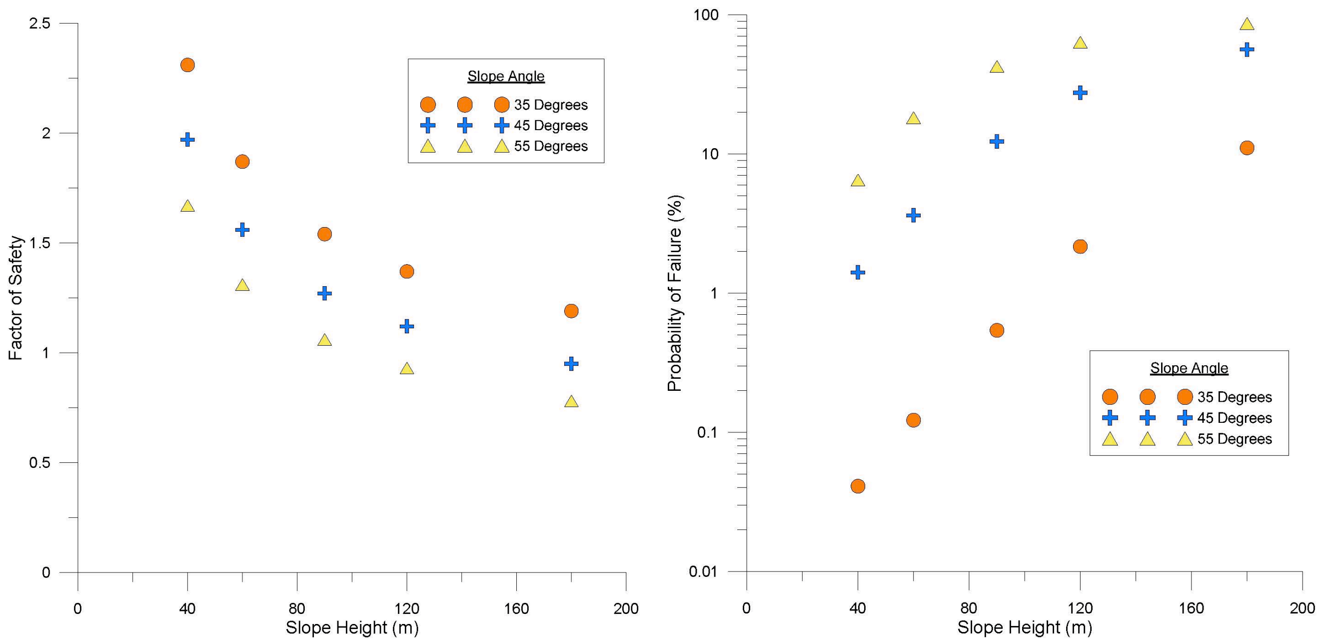

(a) (b)

Figure 10 Plots of a) Slope height versus factor of safety, and b) Slope height versus probability of failure

A scatterplot of FOS versus P_f is shown in Figure 11. Note that there is a wide range of P_f values observed for approximately the same FOS value. Larger slopes tend to have lower P_f values than smaller slopes (for similar FOS values), as shown in Figure 12.

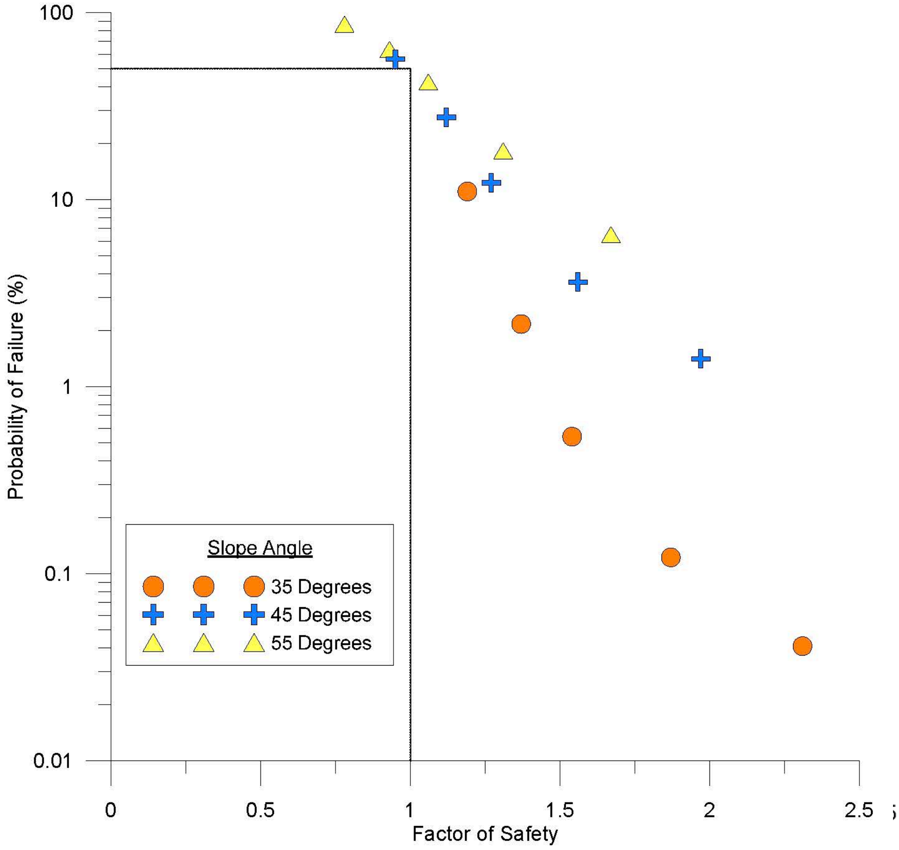

Figure 11 Plot of factor of safety versus probability of failure

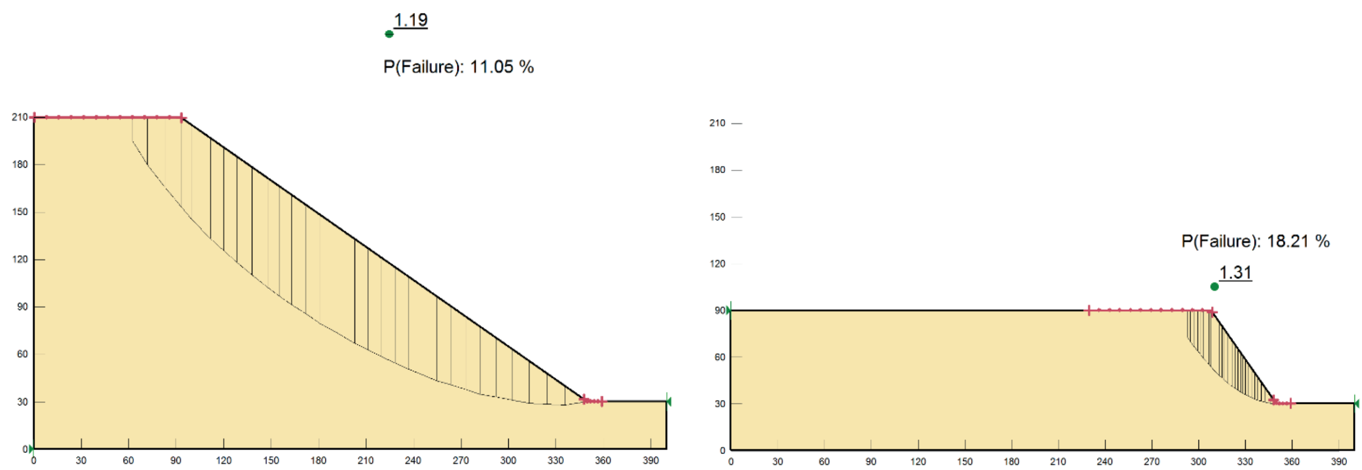

(a) (b)

Figure 12. Results of the probabilistic limit-equilibrium analysis for a) Slope with height of 180 meters and angle of 35 degrees, and b) Slope with height of 60 meters and angle of 55 degrees

5. CONSIDERATIONS AND LIMITATIONS

1. Most large documented slope failures in rock involve at least some structural component. The techniques described in this paper focus on input variables to estimate rock-mass properties. Structural weaknesses still must be considered and incorporated into rock slope analyses. There is no substitute for good engineering judgement in the determination of the critical failure mechanism of a slope.
2. The variogram is also required for block model generation with kriging, and is useful for determining optimum sampling intervals or drill hole spacing (since θ is the average distance between independent samples).

3. The analyses presented in this paper assume an isotropic variogram structure. It is possible that given the inherent anisotropic nature of rock, the variogram may also be anisotropic. This may be tested by performing directional variography (Isaaks and Srivastava, 1989; Cressie, 1991) if sufficient data is available.
4. The variogram should not be estimated from interpolated or extrapolated datasets such as block models. Interpolation techniques may impart the appearance of spatial correlation to a dataset when none may exist.
5. Limit-equilibrium methods may have difficulty locating the critical probabilistic failure surface. The critical deterministic failure surface may not coincide with the critical probabilistic failure surface. Li and Lumb (1987) state that the two critical failure surfaces are typically close to one another, but this is likely dependent on the geometry of the slope and variability of parameters. This potential issue may be overcome with the Random Finite-Element Method (Fenton and Griffiths, 2008) and conditional simulation.
6. For probabilistic analysis, all sources that contribute significant uncertainty to model parameters deserve consideration; this may include additional uncertainty regarding lithological boundaries, alteration boundaries, or pore water pressure. The Large Open Pit study (Read and Stacey, 2009) estimated that it is not uncommon for pore water pressure estimations to be over or under by a factor of 2.
7. Although it may be tempting to directly measure the variance reduction function (instead of estimating θ from the variogram), the measured variance reduction function is very sensitive to the spatial density of the data. The variogram is a more robust estimator of θ in widely spaced data fields, as are typically encountered in geotechnical engineering.
8. Fenton and Griffiths (2008) have noted that it may be non-conservative to assign the arithmetic mean strength to an entire slope model, since the failure path will preferentially develop through the weakest materials. The influence of this effect will depend on θ and the amount of nugget variance.
9. The estimated variance of rock mass strength will also depend upon the proximity of measured data. This effect may be captured through conditional simulation kriging (Isaaks and Srivastava, 1989; Fenton and Griffiths, 2008).

6. CONCLUSIONS

Probabilistic slope analysis requires that assumptions be made regarding the spatial variability of rock strength parameters. If spatial variability is not considered, a probabilistic slope analysis can result in either over- or under-estimation of the probability of failure.

The standard deviation of a measured parameter is not directly applicable to a slope analysis, since it is the average shear strength along a failure surface that controls the strength of a slope and not the 'point-to-point' variability. The variance of a spatial average will always be less than the variance of the individual data points. The variability of the spatially averaged shear strength decreases for increasing spatial average size (or slope size). The variogram and the variance reduction function can be used to quantify how much the variance will be reduced for any spatial average size.

Based on the projects analyzed for this research, it is proposed that the natural variability of intact and fracture shear strength can be disregarded in most cases when the model domain is significantly greater than scale of fluctuation. The statistical uncertainty (variance of the mean) must still be considered even if natural variability is not. If sufficient data is present to plot the variogram for a specific project, it should be verified that the scale of fluctuation is indeed very small relative to the slope analysis.

Equation 2 and Figure 3 account for many factors that influence rock-mass strength uncertainty:

- If a larger spatial average size is analyzed, the long-scale variance (σ^2_V) is reduced correspondingly by the variance reduction function to account for the effect of spatial averaging.
- If more samples are taken to better estimate the input parameters, the variance of the mean is correspondingly reduced.
- If there is calibration to previous excavation performance, the transformation model uncertainty may be reduced.

- The nugget variance (σ^2_N) is reduced to zero for any nominal spatial average size larger than the sample spacing of the data that was used to create the variogram model. This excludes the portion of the variance caused by small-scale variation, inherent randomness, and measurement error.

Another factor that influences the uncertainty of a parameter estimate is the proximity of measured data; conditional simulation kriging is required in order to account for this effect.

Separating the uncertainty of rock-mass parameters into the components of natural variability, statistical uncertainty, and transformation uncertainty better informs the practitioner where to allocate future efforts to have the most impact to reduce uncertainty.

As a standard of practice, the assumptions regarding the spatial correlation of random variables should always be documented and presented alongside probabilistic global slope analyses.

7. ACKNOWLEDGEMENT

The authors thank the many mining companies who provided data for this research.

8. REFERENCES

- Akkaya, A.D., and VanMarcke, E.H. (2003) Estimation of Spatial Correlation of Soil Parameters Based on Data from the Texas A&M University NGES, in Probabilistic Site Characterization at the National Experimentation Sites, ASCE Geotechnical Special Publication, E.H. Van Marcke and G.A. Fenton (eds), No. 121, New York, USA, pp. 29-40.

- Ang, A.G.S., and Tang W.H. (1975) Probability Concepts in Engineering Planning and Design Volume I-Basic Principles, John Wiley & Sons, 409 p.

- Call, R.D., Cicchini, P.F., Ryan, T.M., and Barkley, R.C. (2001) Managing and Analyzing Overall Pit Slopes, in Slope Stability in Surface Mining, Hustrulid, W.A., McCarter, M.K., and Van Zyl, D.J.A. (eds), SME, pp. 39-46.

- Chenari, R., and Dodaran, R. (2010) New methods for estimation of the scale of fluctuation of geotechnical properties in natural deposits, Comp. Meth. In Civil Eng., 1(1), pp. 55-64.

- Chilès, J.P, and Delfiner, P. (2012) Geostatistics: Modeling Spatial Uncertainty, John Wiley & Sons, 699 p.

- Cressie, N.A. (1991) Statistics for Spatial Data, John Wiley & Sons, 920 p.

- Deere D.U., 1968. Geological considerations. Rock Mechanics in Engineering Practice, eds. K.G. Stagg and

- El-Ramly, H., Morgenstern, N.R., and Cruden, D.M. (2002) Probabilistic slope stability analysis for practice, Canadian Geotechnical Journal, 39(3), pp. 665-683.

- Fenton, G.A. (1999) Random Field Modeling of CPT Data, Journal of Geotechnical and Geoenvironmental Engineering, 125(6), pp. 486-498.

- Fenton, G.A., and Griffiths, D.V. (2008) Risk Assessment in Geotechnical Engineering, John Wiley & Sons, 461 p.

- Hoek, E., Carranza-Torres, C.T., and Corkum, B. (2002) Hoek-Brown failure criterion – 2002 edition, in Proceedings of the Fifth North American Rock Mechanics Symposium, Hammah et al. (eds), University of Toronto Press, pp.267-273.

- Hoek, E., Carter, T.G., and Diederichs, M.S. (2013) Quantification of the geological strength index chart, in Proceedings of the 47th Rock Mechanics/Geomechanics Symposium, 23-26 June 2013, San Francisco, CA, American Rock Mechanics Association.

- Isaaks, E.H., and Srivastava, R.M. (1989) An Introduction to Applied Geostatistics, Oxford University Press, 561 p.
- Li, K.S. and Lumb P. (1987) Probabilistic design of slopes, Canadian Geotechnical Journal, 24(4), pp. 520-535.
- Mayer, J.M., and Stead D. (2017) A comparison of traditional, step-path, and geostatistical techniques in the stability analysis of a large open pit. Rock Mechanics and Rock Engineering. 50:927-949.
- Palmstrom, A. (2005) Measurements of and Correlations between Block Size and Rock Quality Designation (RQD), Tunnels and Underground Space Technology, 20, pp. 362-377.
- Phoon, K.K., and Kulhawy, F.G. (1999) Characterization of geotechnical variability, Canadian Geotechnical Journal, 36(4), pp. 612-624.
- Phoon, K.K., and Kulhawy, F.G. (1999) Evaluation of geotechnical property variability, Canadian Geotechnical Journal, 36(4), pp. 625-639.
- Read, J., and Stacey, P. (2009) Guidelines for Open Pit Slope Design, CSIRO Publishing, 510 p.
- Ureel, S.D., Killian, J.R., and Ryan, T.M. (2012) An Analysis to Compare Factor of Safety Values Between the Limit Equilibrium Method and Shear Strength Reduction Technique, Proceedings of 46th US Rock Mechanics / Geomechanics Symposium, Bobet, A. (ed), 24-27 June 2012, Chicago, IL, USA, ARMA, pp. 2852-2858.
- VanMarcke, E.H. (1977) Probabilistic modeling of soil profiles, ASCE Journal of the Geotechnical Engineering Division, 103, pp. 1237-1246.
- Vanmarcke, E.H. (2010) Random Fields: Analysis and Synthesis, World Scientific Publishing, 350 p.
- Wang, J., Tan, W., Feng, S., and Zhou, R. (2000) Reliability analysis of an open pit coal mine slope, International Journal of Rock Mechanics and Mining Sciences, 37, pp. 715-21.
- Wiles, T.D. (2006) Reliability of numerical modelling predictions, International Journal of Rock Mechanics and Mining Sciences, 43, pp. 454-472.